Spring 2015

Multimodal inputs and modularity of the inferior colliculus prior to audition.

Joseph A. Balsamo
James Madison University

Multimodal inputs and modularity of the inferior colliculus prior to audition.

An Honors Program Project Presented to

the Faculty of the Undergraduate

College of Science and Mathematics

James Madison University

by Joseph Anthony Balsamo

May 2015

Accepted by the faculty of the Department of Biology, James Madison University, in partial fulfillment of the requirements for the Honors Program.

FACULTY COMMITTEE:

Project Advisor: Mark L. Gabriele, Ph.D.
Professor, Biology

Reader: Janet C. Daniel, Ph.D.
Associate Professor, Biology

Reader: Tim A Bloss, Ph.D.
Associate Professor, Biology

HONORS PROGRAM APPROVAL:

Philip Frana, Ph.D.,
Interim Director, Honors Program

PUBLIC PRESENTATION

This work is accepted for presentation, in part or in full, at the Association for Otolaryngology 38th Annual Mid-Winter meeting on February 23th, 2015 and at the Central Virginia Chapter of the Society for Neuroscience on March 20th, 2015.

Table of Contents

Acknowledgements

Words cannot express the amount of gratitude and appreciation I have for Dr. Mark Gabriele. No descriptive fillers can describe his role as both a mentor and a friend. His ability to balance his commitments to students, family, and research is a reflection of who he is as a person and a quality I aspire to one-day mirror. He taught me not just lab techniques and critical thinking skills; but how to conduct myself as a scientist and, more importantly, as a person.

Of course, Dr. Gabriele's lab experience would not have been possible without James Madison University and the Biology Department. Special thanks are due to the biology department for providing the necessary funding to attend several conferences. I must also thank my readers Dr. Janet Daniel and Dr. Tim Bloss for valued and timely input throughout the project. I would also like to thank the JMU Honors College for awarding me the Hillcrest Scholarship, affording an incredible opportunity to conduct an off campus research experience, and Dr. Melinda Adams for her outstanding dedication to the program.

To the Gabriele lab members I have learned from as an underclassman, I thank you for your patience and willingness to teach; to those lab members I have worked alongside with, I thank you for unwavering support and scientific curiosities.

I would like to thank God for the opportunities presented to me, my family for their love, and my friends for their laughter. To my parents, Joe and Vicky, thank you for believing in me, raising me, and loving me. To my sisters, Devan and Alexa, thank you for the motivation and inspiration you have provided me throughout my collegiate career. Finally, a thank you to both my grandmothers for keeping me in their prayers.

List of Figures

Disclaimer

The following project is written and organized in accordance with the manuscript submission guidelines for the Journal of Developmental Neurobiology. Additional information can be found at: http://onlinelibrary.wiley.com/journal/10.1002/(ISSN)1932-846X/homepage/ForAuthors.html.

Multimodal Inputs and Modularity of the Inferior Colliculus Prior to Audition.

Joseph Anthony Balsamo, Mark Lawrence Gabriele

Department of Biology, MSC 7801, James Madison University, Harrisonburg, Virginia 22807

Correspondence to:

Mark L. Gabriele, PhD, Professor

Department of Biology

MSC 7801

James Madison University

Harrisonburg, Virginia 22807

phone: 540-568-6333

email: gabrieml@jmu.edu

ABSTRACT

A fully functional nervous system requires assimilation of sensory modalities to adequately interpret stimuli and determine appropriate motor responses. Two such regions responsible for multimodal integration are found in the auditory system, the cochlear nucleus (CN) and the inferior colliculus (IC). The lateral cortex of the IC (LCIC) in particular receives a diverse multimodal input array to discrete modular/extramodular zones. Staining for certain neurochemicals, including GAD, a marker for GABAergic neurons, reveal this compartmentalized LCIC organization. The present study utilizes fluorescent anterograde tract-tracing techniques to determine the development of a somatosensory brainstem projection from the spinal trigeminal nucleus (Sp5), to multimodal aspects of the CN and LCIC. The results indicate somatosensory innervation of these structures parallels that of developing auditory afferents and that auditory-somatosensory convergence described in the adult in these areas is likely set prior to acoustic experience. Immunohistochemical GAD staining and expression studies for molecular guidance molecules (EphA4, ephrin-B2, ephrin-B3) reveal early LCIC modularity during the period of bimodal projection shaping. Such findings suggest an emergence of LCIC domains early in development that may in part be guided by Eph-ephrin protein interactions. Understanding the neuronal development of converging auditory and somatosensory maps is essential for understanding their presumed roles in suppression of self-generated sounds. Furthermore, a sound foundation for mechanisms guiding multimodal input array formation is necessary to improve noninvasive interactions that aim to reset maladaptive map plasticity underlying debilitating conditions like tinnitus.

Keywords: inferior colliculus, GAD, somatosensory, auditory, multimodal

INTRODUCTION

The auditory system is primarily responsible for deciphering complex sound characteristics such as pitch, frequency, and intensity. Interpreting precise signal attributes and computation of complex tasks requires multiple processing centers and cross communication among different sensory modalities. The inferior colliculus (IC), located in the auditory midbrain, is one such processing area classically described as an auditory relay hub. The three subdivisions of the IC, the central nucleus (CNIC), lateral cortex (LCIC), and dorsal cortex (DCIC) (Faye-Lund and Osen, 1985; Loftus et al., 2008), have been investigated to varying degrees. Well characterized is the tonotopic input array to the CNIC from other auditory centers (Merzenich and Reid, 1974; Roth et al., 1978; Semple and Aitkin, 1979; Schreiner and Langner, 1988; Kandler et al., 2009) resulting in distinct laminar inputs that are frequency dependent.

Although such frequency mapping is ideal for purely auditory nuclei, interpreting coded information in characteristic frequencies, this model appears less appropriate for multisensory regions within the auditory pathway. For example, the cochlear nucleus (CN) receives auditory input from the cochlea (Nelken, 2008) as well as somatosensory afferents from trigeminal ganglion (TG), dorsal column nuclei: cuneate (Cu) and gracilis (Gr), and spinal trigeminal nucleus (Sp5) (Itoh et al., 1987; Wright and Ryugo, 1996; Zhou and Shore, 2004; Haenggeli et al., 2005). Similarly, the LCIC not only receives auditory innervation from auditory cortex (AC), CN and CNIC (Aitkin et al., 1981; Ryugo et al., 1981; Saldaña and Merchán, 1992; Malmierca et al., 1995; Saldaña et al., 1996; Zhou and Shore, 2006) but also somatosensory innervation from Cu, Gr, and Sp5 across a variety of adult species including rat, cat, guinea pig, and monkey (RoBards et al., 1976; Robards, 1979; Coleman and Clerici, 1987; Wiberg et al., 1987; Weinberg and Rustioni, 1989; Shore and Zhou, 2006; Zhou and Shore, 2006). The LCIC cytoarchitecture is

not defined by distinct frequency laminae like its CNIC counterpart, but rather as modular (layer 2) and extramodular (layers 1 & 3) zones as exhibited by a host of neurochemical expression patterns (Chernock et al., 2004; Hilbig et al., 2007, Lesicko and Llano, 2015).

While LCIC connectivity and neurochemical modularity has been described in adults, analogous studies regarding the emergence of modular fields and patterning of multimodal inputs are largely lacking. To date, there exist only a handful of studies that address auditory inputs to the LCIC. CN projects bilaterally to layer 2 LCIC modular zones extending into rostral extremes of the subdivision (Kandler and Friauf, 1993). Complementary to this pattern, descending inputs from AC (Torii et al., 2013) and intrinsic connections from the neighboring CNIC (Noftz et al., 2014) (Figure 1) project primarily to ipsilateral, extramodular LCIC domains and are established prior to hearing onset.

In terms of developing somatosensory afferents to the LCIC, even less is known. Adult data regarding somatosensory LCIC inputs have focused on projections arising from Sp5 (Zhou and Shore, 2004, 2006; Shore and Zhou, 2006), which encodes proprioceptive information from facial, oral and vocal cord structures (Romfh et al., 1979; Capra, 1987; Jacquin et al., 1989; Nazruddin et al., 1989; Takemura et al., 1991; Suemune et al., 1992), and dorsal column nuclei, responsible for proprioceptive contributions from the limbs (RoBards et al., 1976; Coleman and Clerici, 1987; Wiberg et al., 1987; Weinberg and Rustioni, 1989; Hilbig et al., 2007). Pathways from the aforementioned somatosensory nuclei in adult species are primarily contralateral and target discrete LCIC modular fields (RoBards et al., 1976; Coleman and Clerici, 1987; Wiberg et al., 1987; Weinberg et al., 1989; Zhou and Shore, 2006; Hilbig et al., 2007). These patchy, discontinuous layer 2 patterns in the adult appear to be segregated largely with regard to heavy auditory inputs from AC and CNIC that preferentially terminate in layers 1 and 3 (Lesicko and

Llano, 2015).

The present study identifies an early somatosensory input from Sp5 to LCIC in newborn mouse. We discuss the timing of developing Sp5 inputs with that of emerging auditory afferents and LCIC modularity assessed by GAD staining and Eph-ephrin guidance protein localization.

MATERIALS AND METHODS

Animals

Experiments were performed on C57BL/6J control mice (Jackson Laboratories, Bar Harbor, ME) prior to hearing onset at various postnatal ages (n = 9) in keeping with previously described time points for topographic inputs to the IC (Gabriele et al., 2000, 2007, 2011; Henkel et al., 2005; Fathke and Gabriele, 2009; Wallace et al., 2013). All experimental procedures were performed in compliance with National Institutes of Health *Guide for the Care and Use of Laboratory Animals* (NIH Publications No. 80-23, revised 1996) and received prior approval from the Institutional Animal Care and Use Committee.

NeuroVue Tracing of Sp5-IC Projections

Postnatal mice were given an overdose of ketamine (200 mg/kg) and xylazine (20 mg/kg) and perfused through the heart (physiological rinse followed by 4% paraformaldehyde solution, pH 7.4). Brains were removed from the skull and post-fixed overnight at 4°C in paraformaldehyde fixative solution. Post-fixed tissue was blocked in the coronal plane just rostral to superior colliculus (SC) and caudally at the spinal cord brainstem junction before embedding (5 ml 8% gelatin in dH_2O/10 ml egg yolk). Brains were then sectioned caudal to rostral at 75 μm on a Vibratome until Sp5 could be identified with brightfield microscopy. Slivers of lipophilic dye-soaked filter paper (Molecular Targeting Technologies, West Chester, PA) were cut with Micro-

Vannas surgical scissors with the aid of a dissecting microscope and were then placed in Sp5. It should be noted even with the care and precision taken with each dye placement that variations exist among cases regarding precise location and amount of dye delivered. Tissue blocks were incubated at 37°C for 1 month in the dark to facilitate dye diffusion. Fixative solution was replaced every two weeks to maintain tissue integrity. After incubating, the remaining block of tissue was sectioned at 75 μm and counterstained with bis-benzamide nuclear counterstain (Hoechst 33258; Invitrogen, Carlsbad, CA) for 5 min to visualize Sp5 and IC cytoarchitecture. Sections were rinsed 3x for 5 min in PBS, mounted, and coverslipped while wet with GelMount (BioMeda, Foster City, CA).

GAD Immunohistochemistry

Animals were perfused as described above with an additional fixation step using 4% paraformaldehyde, 10% sucrose solution (pH 7.4). Brains were then removed and post-fixed overnight in the same solution followed by an additional overnight cryoprotection in 4% paraformaldehyde, 30% sucrose solution (pH 7.4). 50 μm thick sections were taken on a sliding-freezing microtome in the coronal plane. Tissue processing began with an endogenous quench (3% H_2O_2 in PBS) of peroxidase activity for 5 min followed by three, 5 min PBS rinses. A 30 min protein-blocking step (2.5 % Normal Horse Serum) followed, conducted at room temperature. Primary rabbit anti-GAD (Millipore AB1511 1:3000) was applied overnight at 4°C. This antibody labels both cellular GAD isoforms (67 & 65 respectively). Tissue was then equilibrated to room temperature and rinsed 3x for 5 min in PBS. Sections were then incubated at room temperature in an anti-rabbit IMPRESS reagent kit made in horse (Vector Laboratories MP-7401 IMPRESS reagent kit). An additional three PBS rinses for 5 min preceded incubation with ABC-DAB reaction kit (Vector Laboratories SK-4100). Sections were then rinsed 3x for 5

min in PBS and mounted on gelatin-subbed slides. Sections were rehydrated briefly in dH_2O before being passed through a series of alcohol washes (50%, 70 %, 95%, 2x at 100%, for 10 min each) and two, 10 min xylene clearing steps. Slides were coverslipped with Vecta-mount mounting media (Vector H-5000).

Microscopy and Image Capture

A monochrome cooled CCD CoolSnap HQ digital camera (Roper Scientific, Tuscon, AZ) and a Nikon TE 2000 microscope (Nikon, Melville, NY) were used to capture fluorescent images. R and B Phycoeythrin (NueroVue) and DAPI (bis-benzamide) filter sets (ChromaTechnology, Brattleboro, VT) were used to visualize both molecules. Two monochrome channels were acquired, merged digitally, and pseudocolored (green: NeuroVue axonal labeling; blue: bis-benzamide nuclear counterstain).

Magnification series were collected throughout the rostrocaudal extent of the IC for Sp5 dye labeling. For images 10x and higher Z-stacks were acquired to capture focused labeling throughout the entire 75 μm thick section. Three-dimensional Z-stacks (Elements Software; Nikon) were flattened into two dimensions using a maximum projection algorithm. Images were saved as JPEG 2000 files. Brightness/contrast values were manipulated in some cases for illustration purposes or to emphasize the bis-benzamide channel to assist in drawing cytoarchitectural boundaries (Adobe Photoshop, San Jose, CA).

GAD image capture was performed using brightfield microscopy with a Nikon Digital Sight Color Camera using DSFi1 filter set (Nikon, Melville, NY). White balances were performed on image series captured at 4x, 10x, 20x, 40x, and 60x (Adobe Photoshop, San Jose, CA).

RESULTS

Sp5 Dye Placements

Sticks were localized in Sp5. Additionally, variation in dorsal or ventral placements were made in an effort to establish Sp5-LCIC topography; however, these attempts revealed no obvious trends in these early connections. As such, neither ventral nor dorsal dye placements show more robust input to LCIC or targeting of spatially distinct LCIC regions. Rather, dye placement size was the critical factor in the number of labeled inputs with larger placements revealing more axon fibers. It should be noted that in all cases, Sp5 dye placements resulted in backfilling of the spinal trigeminal tract (sp5), thereby confirming placement in Sp5 nucleus (Figure 2).

Sp5 Projections to CN

Anterograde experiments from Sp5 reveal inputs to anteroventral cochlear nucleus (AVCN) at P4 (Figure 3) and maintained at P8. At both ages inputs were ipsilateral dominant with heaviest terminal fields in AVCN marginal zones (Figure 3), as has been described in adult guinea pig (Zhou and Shore, 2004).

Sp5 Projections to LCIC

Sp5 sends afferent projections bilaterally to LCIC during circuitry development (Figure 4). Fiber trajectory was consistent in all cases at all ages (Figure 5). Labeled contralateral fibers ascend for a short distance before crossing the midline and passing just dorsal to the lateral superior olive (LSO) (Figure 5, A). Fibers then enter the IC (Figure 5, B) and project to medial, lateral, or rostral LCIC regions (Figures 6 & 7). Interestingly, rostral regions of LCIC, caudal to intertegmental nucleus (ITN), receive the heaviest inputs in all cases and show increased axonal

branching compared to medial and lateral aspects of the LCIC (Figure 7).

While synaptic inputs are present at P0 (Figure 4), no clear organization of Sp5 fibers into LCIC modular fields was observed. Similarly, Sp5 projection patterns at P4, while substantial, still showed no obvious specificity regarding projection distribution. At P8, preliminary observations suggest some refinement, but discrete modular organization of axonal afferents remains lacking. Further experimentation at slightly older developmental stages should determine when Sp5 inputs to LCIC organize into distinct layer 2 modules.

GAD Immunohistochemistry

GAD immunohistochemistry reveals GABAergic modules at P4 in LCIC (Figure 8). The GAD-positive area present in layer 2 (Figure 8, B) contains positive soma and terminal puncta (Figure 8, C) indicative of GABAergic input and output. These findings suggest an early modular LCIC organization despite lack of patchy somatosensory inputs at these ages.

DISCUSSION

This study presents the first developmental time course for somatosensory innervation to the CN and IC. While these nuclei receive somatosensory and auditory input at similar developmental stages, the emergence of somatosensory patterns (i.e. modules) appears to be delayed relative to auditory pattern formation. In addition we show neurochemical evidence for GAD-positive zones during development suggesting adult neurochemical expression patterns form during the critical period prior to hearing onset.

Dye Placements and Fiber Trajectory

Placements in Sp5 reveal fiber trajectories consistent with mature circuitry in guinea pig (Zhou and Shore, 2004, 2006), cat (Wiberg et al., 1986), and monkey (Wiberg et al., 1987) albeit in dissimilar proportions. These adult trajectories are predominantly contralateral, whereas our developmental findings suggest bilateral pathways. It remains to be determined if aspects of the observed ipsilateral projections are subsequently refined at later developmental stages or with experience.

Of particular note is the contralateral fiber trajectory at the level of LSO (Figure 5, A). Axonal fibers pass dorsal to this nucleus before entering the lateral lemniscus (LL) en route to the IC. Previously, we described LCIC modular input from LSO (Wallace et al., 2013). Considering the fiber trajectory of somatosensory pathways and dye placements reviewed in Wallace (2013), the described modular input in LCIC was likely due to clipping of adjacent somatosensory fibers from Sp5 (Itoh et al., 1987; Wiberg et al., 1987; Jain and Shore, 2006; Zhou and Shore, 2006, present study) and perhaps dorsal column nuclei (Robards, 1979; Coleman and Clerici, 1987; Weinberg and Rustioni, 1987; Wiberg et al., 1987; Weinberg et al., 1989).

Also worth mentioning are the retrogradely labeled ipsilateral cell bodies of the mesencephalic nucleus (Me5) observed in all cases regardless of age (Figure 6, A). Me5 targets upper cervical spinal cord areas via sp5 tract (Veazey and Severin, 1980; Raappana and Arvidsson, 1993; Pombal et al., 1997). Based on the close proximity of sp5 tract to Sp5 nucleus, dye likely diffused into the sp5 tract labeling Me5 cells via their efferent axons.

Projections to CN

Anterograde tracing studies from Sp5 reveal ipsilateral dominant projections to AVCN (Figure 3) consistent with findings in adult guinea pig (Zhou and Shore, 2004). The described projection pattern through the sp5 tract is also conserved for fibers terminating in AVCN marginal zones (Zhou and Shore, 2004) suggesting mammalian continuity in pathway formation and that such pathways are established early in development. Zhou and Shore (2004) also presents terminal puncta labeling in dorsal cochlear nucleus (DCN) and posterior ventral cochlear nucleus (PVCN). Such projection patterns are lacking in our developmental mouse cases and require additional trials to identify such pathways. CN also receives descending auditory input from the superior olivary complex (SOC) and CNIC (Shore et al., 1991) as well as reciprocal connections with the opposing CN (Shore et al., 1992). Thus, auditory and somatosensory convergence may provide a multimodal center allowing for better sound source localization based on proprioceptive information.

Projections to LCIC

Early developmental bilateral terminal fields in LCIC lack defined modular input arrangements. Axon bundles approach the CNIC, before deferring to medial, lateral, or rostral zones. This preference for termination in LCIC regions is consistent in adult species (Wiberg et al., 1986, 1987; Zhou and Shore, 2006), yet inconsistencies arise when comparing projection laterality. Adult studies in cat (Wiberg et al., 1986), monkey (Wiberg et al., 1987), and guinea pig (Zhou and Shore, 2006) yield contralateral projections from Sp5 to LCIC forming conserved modular distribution patterns in layer 2. At birth (Figure 4), and as late as P8, substantial ipsilateral LCIC inputs from Sp5 persist. It remains to be seen whether ipsilateral inputs are pruned in later

developmental stages as contralateral terminations elaborate and organize into discrete modular distributions.

The heaviest labeling at all developmental ages was present in rostral LCIC just caudal to ITN (Figure 7) in line with findings in monkey (Wiberg et al., 1987). This transitional region is a pathway for a variety of sensory afferents to multimodal regions of SC. Therefore fibers from Sp5 may not only be terminating in LCIC but also passing through this nucleus en route to SC. However, clear varicosities on Sp5 axonal labeling in the LCIC suggest, at the very least, synaptic collaterals terminating in multimodal aspects of the LCIC.

The presence of auditory and somatosensory innervation of the LCIC supports a multisensory integration theory. In adult species ascending, horizontal, and descending auditory inputs terminate in layers 1 and 3 of LCIC (Ryugo et al., 1981; Saldaña and Merchán, 1992; Malmierca et al., 1995; Saldaña et al., 1996; Lesicko and Llano, 2015) with the exception of CN terminal zones in layer 2 (Zhou and Shore, 2006). The investigations regarding these same pathways during development reveals similar results (Kandler and Friauf, 1993; Gabriele et al., 2000; Torii et al., 2013, Noftz et al., 2014). Evidence of a multimodal topographic map in LCIC becomes evident when combining auditory and somatosensory input arrays (Figure 9). Moreover, developmental studies of auditory connectivity coupled with the results of this study imply this map forms before hearing onset.

The exact developmental time course for this proposed multimodal map remains to be established. Evidence presented here indicates somatosensory afferents from Sp5 are present at birth but are not completely refined as late as P8. It is likely continued modification of these inputs occurs between P8 and P12 based on fine-tuning of auditory inputs to the CNIC during this developmental window (Fathke and Gabriele, 2009). After discovering the post natal age at

which developmental Sp5 inputs to LCIC matches adult anatomy, double-labeling studies of auditory and somatosensory innervation of LCIC may reveal spatial and temporal relationships of the multisensory contributions to this region. This proposed study could potentially reveal if one sensory modality plays a role in coordinating the inputs of another.

Eph-ephrin Expression Patterns and Axon Terminal Fields

Our lab has also characterized modular/extramodular expression of Eph-ephrin signaling proteins reminiscent of reported adult neurochemically defined LCIC modules. This family of receptor tyrosine kinase signaling proteins utilize bidirectional signaling to encode place maps for complex sensory and motor systems prior to experience (Flanagan and Vanderhaeghen, 1998; Wilkinson, 2001; Cowan and Henkemeyer, 2002; Kullander and Klein, 2002). Within the LCIC EphA4 and ephrin-B2 expression patterns are isolated in layer 2 modules while ephrin-B3 demonstrates extramodular expression in layers 1 and 3 (Noftz et al., 2014) (Figure 10).

Considering known developmental roles in other systems it is plausible Eph-ephrins present in the LCIC coordinate formation of discrete multimodal maps within this IC subdivision. When comparing expression data with differing sensory terminal fields it appears dissimilar sensory inputs localize to specific Eph-ephrin territories. Experiments consisting of Eph-ephrin mutant animal studies could support this theory thus providing valuable insights into mechanisms underlying the establishment of LCIC architecture.

GAD Expression

Neurochemical markers have proven helpful in revealing LCIC layers and modular/extramodular fields. GAD expression patterns characterized in adult rat (Chernock et al., 2004) and mouse (Lesicko and Llano, 2015) reveal distinct layer 2 modules. Here, we show GAD-positive zones

as early as P4 in LCIC (Figure 8). Intriguingly, GAD-positive cell bodies and terminal puncta are apparent (Figure 8, C) in agreement with findings in guinea pig (Nakamoto et al., 2014).

GAD-positive modules at P4, while present, are not yet completely distinct entities. It is likely that separation of modules occurs after P4 as observed for Eph-ephrin modular expression (Gabriele et al., 2011). Furthermore, it is not known whether Eph-ephrin and GAD-positive manifestations colocalize, interdigitate, or overlap. Multiple labeling studies for both neurochemicals can provide useful perception regarding the compartmentalization of the LCIC and whether they serve as a substrate for input-output arrays.

LCIC Functionality

The LCIC responds to complex auditory stimuli across a broadly tuned spectrum (Aitkin et al., 1975, 1981, 1994; Aitkin and Zimmermann, 1978; Syka et al., 2000; Suta et al., 2003; Ota et al., 2004) in addition to somatosensory stimuli (Aitkin and Zimmermann, 1978; Aitkin et al., 1981). Direct electrical stimulation to Sp5 (Zhou and Shore, 2004) also induces LCIC responses. Even so, understanding the functional significance of Sp5 projections to LCIC requires an appreciation for known Sp5 inputs. Facial and oral structures, such as the vocal tract, tongue, and jaw convey proprioceptive information (Romfh et al., 1979; Capra, 1987; Jacquin et al., 1989; Nazruddin et al., 1989; Takemura et al., 1991; Suemune et al., 1992) to Sp5 via the TG (Dehmel et al., 2008). Combining these findings with LCIC innervation from Sp5 provides a polysynaptic pathway that may be responsible for proprioceptive sensory input to the LCIC from body regions responsible for sound production. Therefore, Sp5 inputs to LCIC GABAergic zones, originating from intra-oral structures, could act as a priming mechanism for the presence of self-made vocalization, which may in turn activate inhibitory pathways that selectively suppress certain primary circuits

tuned to voice-specific characteristics consequently increasing attentiveness to non-self auditory stimuli.

Potential for Tinnitus Treatment

Tinnitus, or the perception of a non-existent auditory stimulus, is a debilitating disease affecting millions of Americans. In addition to age related tinnitus onset, somatic tinnitus can occur due to plastic changes in neural circuitry. This particular type of tinnitus is not marked by aging but rather changes in somatosensory inputs affecting the central gain in auditory pathways (Levine, 1999; Eggermont, 2005; Saunders, 2007). Such changes in mapping can be attributed to whiplash, temperomandibular joint syndrome, or bruxism. Understanding the normal anatomy behind properly functioning sensory circuits can provide insights to anatomical deviation in tinnitus disease states. At the same time, knowing somatosensory circuitry can cause auditory dysfunction offers potential to exploit somatosensory pathways to alleviate symptoms. For example, stimulation on the skin at the level of C2 vertebrae activates a polysynaptic circuit that passes through Sp5 and onward to LCIC. Consistent stimulus at C2 could therefore change affected topography back to a normal conformation ultimately achieving tinnitus relief. Finding other somatosensory regions that innervate auditory modalities could aid in field progression of tinnitus treatment.

ACKNOWLEDGMENTS

Grant sponsor: National Institutes of Health; Grant number: DC012421-01; Grant sponsor: Commonwealth Research Board; Grant number: 06-09; Grant sponsor: National Science Foundation; Grant number: DBI-0619207.

REFERENCES

Aitkin L, Tran L, Syka J. 1994. The responses of neurons in subdivisions of the inferior colliculus of cats to tonal, noise and vocal stimuli. Exp brain Res 98:53–64.

Aitkin LM, Kenyon CE, Philpcyl PT, Philpott P. 1981. The Representation of the Auditory and Somatosensory Systems in the External Nucleus of the Cat Inferior Colliculus. J Comp Neurol 40:25–40.

Aitkin LM, Webster WR, Veale JL, Crosby DC. 1975. Inferior colliculus. I. Comparison of response properties of neurons in central, pericentral, and external nuclei of adult cat. J Neurophysiol 38:1196–1207.

Aitkin LM, Zimmermann M. 1978. External Nucleus of Inferior Colliculus : Auditory and Spinal Somatosensory Merents and Their Interactions. 41.

Capra NF. 1987. Localization and central projections of primary afferent neurons that innervate the temporomandibular joint in cats. Somatosens Res 4:201–13.

Chernock ML, Larue DT, Winer JA. 2004. A periodic network of neurochemical modules in the inferior colliculus. Hear Res 188:12–20.

Coleman JR, Clerici WJ. 1987. Sources of projections to subdivisions of the inferior colliculus in the rat. J Comp Neurol 262:215–226.

Cowan CA, Henkemeyer M. 2002. Ephrins in reverse, park and drive. Trends Cell Biol 12:339–46.

Dehmel S, Cui YL, Shore SE. 2008. Cross-modal interactions of auditory and somatic inputs in the brainstem and midbrain and their imbalance in tinnitus and deafness. Am J Audiol 17:S193–209.

Eggermont JJ. 2005. Tinnitus: neurobiological substrates. Drug Discov Today 10:1283–90.

Fathke RL, Gabriele ML. 2009. Patterning of multiple layered projections to the auditory midbrain prior to experience. Hear Res 249:36–43.

Faye-Lund H, Osen KK. 1985. Anatomy of the inferior colliculus in rat. Anat Embryol (Berl) 171:1–20.

Flanagan JG, Vanderhaeghen P. 1998. The ephrins and Eph receptors in neural development. Annu Rev Neurosci 21:309–45.

Gabriele ML, Brubaker DQ, Chamberlain KA, Kross KM, Simpson NS, Kavianpour SM. 2011. EphA4 and ephrin-B2 expression patterns during inferior colliculus projection shaping prior to experience. Dev Neurobiol 71:182–99.

Gabriele ML, Brunso-Bechtold JK, Henkel CK. 2000. Development of afferent patterns in the inferior colliculus of the rat: projection from the dorsal nucleus of the lateral lemniscus. J Comp Neurol 416:368–82.

Gabriele ML, Shahmoradian SH, French CC, Henkel CK, McHaffie JG. 2007. Early segregation of layered projections from the lateral superior olivary nucleus to the central nucleus of the inferior colliculus in the neonatal cat. Brain Res 1173:66–77.

Haenggeli C-A, Pongstaporn T, Doucet JR, Ryugo DK. 2005. Projections from the spinal trigeminal nucleus to the cochlear nucleus in the rat. J Comp Neurol 484:191–205.

Henkel CK, Gabriele ML, McHaffie JG. 2005. Quantitative assessment of developing afferent patterns in the cat inferior colliculus revealed with calbindin immunohistochemistry and tract tracing methods. Neuroscience 136:945–55.

Hilbig H, Nowack S, Boeckler K, Bidmon H-J, Zilles K. 2007. Characterization of neuronal subsets surrounded by perineuronal nets in the rhesus auditory brainstem. J Anat 210:507–17.

Itoh K, Kamiya H, Mitani A, Yasui Y, Takada M, Mizuno N. 1987. Direct projections from the dorsal column nuclei and the spinal trigeminal nuclei to the cochlear nuclei in the cat. Brain Res 400:145–150.

Jacquin MF, Barcia M, Rhoades RW. 1989. Structure-function relationships in rat brainstem subnucleus interpolaris: IV. Projection neurons. J Comp Neurol 282:45–62.

Jain R, Shore S. 2006. External inferior colliculus integrates trigeminal and acoustic information: unit responses to trigeminal nucleus and acoustic stimulation in the guinea pig. Neurosci Lett 395:71–5.

Kandler K, Clause A, Noh J. 2009. Tonotopic reorganization of developing auditory brainstem circuits. Nat Neurosci 12:711–7.

Kandler K, Friauf E. 1993. Pre- and postnatal development of efferent connections of the cochlear nucleus in the rat. J Comp Neurol 328:161–84.

Kullander K, Klein R. 2002. Mechanisms and functions of Eph and ephrin signalling. Nat Rev Mol Cell Biol 3:475–86.

Levine RA. Somatic (craniocervical) tinnitus and the dorsal cochlear nucleus hypothesis. Am J Otolaryngol 20:351–62.

Lesicko AMH and Llano DA. 2015. Connectional and neurochemical modularity of the mouse inferior colliculus. Assoc Res Otolaryngology Mtg, PS-564.

Loftus WC, Malmierca MS, Bishop DC, Oliver DL. 2008. The cytoarchitecture of the inferior colliculus revisited: a common organization of the lateral cortex in rat and cat. Neuroscience 154:196–205.

Malmierca MS, Rees A, Le Beau FE, Bjaalie JG. 1995. Laminar organization of frequency-defined local axons within and between the inferior colliculi of the guinea pig. J Comp Neurol 357:124–44.

Merzenich MM, Reid MD. 1974. Representation of the cochlea within the inferior colliculus of the cat. Brain Res 77:397–415.

Nakamoto KT, Mellott JG, Killius J, Storey-Workley ME, Sowick CS, Schofield BR. 2014. Ultrastructural characterization of GABAergic and excitatory synapses in the inferior colliculus. Front Neuroanat 8:108.

Nazruddin, Suemune S, Shirana Y, Yamauchi K, Shigenaga Y. 1989. The cells of origin of the hypoglossal afferent nerves and central projections in the cat. Brain Res 490:219–35.

Nelken I. 2008. Processing of complex sounds in the auditory system. Curr Opin Neurobiol 18:413–7.

Noftz WA, Gray LC, Gabriele ML. 2014. Converging midbrain afferent patterns and auditory brainstem responses in ephrin-B3 mutant mice. Assoc Res Otolaryngology Mtg, PS-070.

Ota Y, Oliver DL, Dolan DF. 2004. Frequency-specific effects on cochlear responses during activation of the inferior colliculus in the Guinea pig. J Neurophysiol 91:2185–93.

Pombal MA, Alvarez-Otero R, Rodicio MC, Anadónt R. 1997. A tract-tracing study of the central projections of the mesencephalic nucleus of the trigeminus in the guppy (Lebistes reticulatus, Teleostei), with some observations on the descending trigeminal tract. Brain Res Bull 42:111–118.

Raappana P, Arvidsson J. 1993. Location, morphology, and central projections of mesencephalic trigeminal neurons innervating rat masticatory muscles studied by axonal transport of choleragenoid-horseradish peroxidase. J Comp Neurol 328:103–14.

RoBards MJ, Watkins DW, Masterton RB. 1976. An anatomical study of some somesthetic afferents to the intercollicular terminal zone of the midbrain of the opossum. J Comp Neurol 170:499–524.

Robards MJ. 1979. Somatic neurons in the brainstem and neocortex projecting to the external nucleus of the inferior colliculus: an anatomical study in the opossum. J Comp Neurol 184:547–65.

Romfh JH, Capra NF, Gatipon GB. 1979. Trigeminal nerve and temporomandibular joint of the cat: A horseradish peroxidase study. Exp Neurol 65:99–106.

Roth GL, Aitkin LM, Andersen RA, Merzenich MM. 1978. Some features of the spatial organization of the central nucleus of the inferior colliculus of the cat. J Comp Neurol 182:661–80.

Ryugo DK, Willard FH, Fekete DM. 1981. Differential afferent projections to the inferior colliculus from the cochlear nucleus in the albino mouse. Brain Res 210:342–349.

Saldaña E, Feliciano M, Mugnaini E. 1996. Distribution of descending projections from primary auditory neocortex to inferior colliculus mimics the topography of intracollicular projections. J Comp Neurol 371:15–40.

Saldaña E, Merchán MA. 1992. Intrinsic and commissural connections of the rat inferior colliculus. J Comp Neurol 319:417–37.

Saunders JC. 2007. The role of central nervous system plasticity in tinnitus. J Commun Disord 40:313–34.

Schreiner CE, Langner G. 1988. Periodicity coding in the inferior colliculus of the cat. II. Topographical organization. J Neurophysiol 60:1823–1840.

Semple MN, Aitkin LM. 1979. Representation of sound frequency and laterality by units in central nucleus of cat inferior colliculus. J Neurophysiol 42:1626–1639.

Shore SE, Godfrey DA, Helfert RH, Altschuler RA, Bledsoe SC. 1992. Connections between the cochlear nuclei in guinea pig. Hear Res 62:16–26.

Shore SE, Helfert RH, Bledsoe SC, Altschuler RA, Godfrey DA. 1991. Descending projections to the dorsal and ventral divisions of the cochlear nucleus in guinea pig. Hear Res 52:255–68.

Shore SE, Zhou J. 2006. Somatosensory influence on the cochlear nucleus and beyond. Hear Res 216-217:90–9.

Suemune S, Nishimori T, Hosoi M, Suzuki Y, Tsuru H, Kawata T, Yamauchi K, Maeda N. 1992. Trigeminal nerve endings of lingual mucosa and musculature of the rat. Brain Res 586:162–165.

Suta D, Kvasnák E, Popelár J, Syka J. 2003. Representation of species-specific vocalizations in the inferior colliculus of the guinea pig. J Neurophysiol 90:3794–808.

Syka J, Popelár J, Kvasnák E, Astl J. 2000. Response properties of neurons in the central nucleus and external and dorsal cortices of the inferior colliculus in guinea pig. Exp brain Res 133:254–66.

Takemura M, Sugimoto T, Shigenaga Y. 1991. Difference in central projection of primary afferents innervating facial and intraoral structures in the rat. Exp Neurol 111:324–31.

Torii M, Hackett TA, Rakic P, Levitt P, Polley DB. 2013. EphA signaling impacts development of topographic connectivity in auditory corticofugal systems. Cereb Cortex 23:775–85.

Veazey RB, Severin CM. 1980. Efferent projections of the deep mesencephalic nucleus (pars medialis) in the rat. J Comp Neurol 190:245–58.

Wallace MM, Kavianpour SM, Gabriele ML. 2013. Ephrin-B2 reverse signaling is required for topography but not pattern formation of lateral superior olivary inputs to the inferior colliculus. J Comp Neurol 521:1585–97.

Weinberg RJ, Rustioni A, Hill C, Carolina N. 1989. Brainstem Projections to the Rat Cuneate Nucleus. 156:142–156.

Weinberg RJ, Rustioni A. 1987. A cuneocochlear pathway in the rat. Neuroscience 20:209–219.

Weinberg RJ, Rustioni A. 1989. Brainstem projections to the rat cuneate nucleus. J Comp Neurol 282:142–56.

Wiberg M, Westman J, Blomqvist A. 1986. The projection to the mesencephalon from the sensory trigeminal nuclei. An anatomical study in the cat. Brain Res 399:51–68.

Wiberg M, Westman J, Blomqvist A. 1987. Somatosensory projection to the mesencephalon: an anatomical study in the monkey. J Comp Neurol 264:92–117.

Wilkinson DG. 2001. Multiple roles of EPH receptors and ephrins in neural development. Nat Rev Neurosci 2:155–64.

Wright DD, Ryugo DK. 1996. Mossy fiber projections from the cuneate nucleus to the cochlear nucleus in the rat. J Comp Neurol 365:159–72.

Zhou J, Shore S. 2004. Projections from the trigeminal nuclear complex to the cochlear nuclei: a retrograde and anterograde tracing study in the guinea pig. J Neurosci Res 78:901–7.

Zhou J, Shore S. 2006. Convergence of spinal trigeminal and cochlear nucleus projections in the inferior colliculus of the guinea pig. J Comp Neurol 495:100–12.

Figure Legends

Figure 1. A. Anterograde, ipsilateral labeling at P8 from CNIC to LCIC layers 1 and 3. Modular zones in layer 2 (*dashed contours*) are devoid of input and are known to receive somatosensory input in the adult. Scale bar = 500 μm.

Figure 2. A. Dye placement in left Sp5. Retrograde filling of axons in the sp5 tract (*lateral region, dashed contour*) confirm accurate placement in Sp5 nucleus. Scale bar = 500 μm.

Figure 3. A. Projections from Sp5 to ipsilateral AVCN are present at P4. Terminal fibers form connections in marginal zones (*inset arrow*). Scale bar = 500 μm.

Figure 4. Bilateral terminations of Sp5 inputs to LCIC at P0. Arrows indicate terminal axons. **A.** Fibers enter medial and lateral regions of the LCIC, yet the majority project to lateral LCIC aspects. **B.** Contralateral labeling is present but not as robust as the ipsilateral side. Terminations still prefer medial and lateral areas of the LCIC. Scale bars = 200 μm.

Figure 5. Contralateral fiber trajectory for projecting fibers from Sp5 en route to LCIC. **A.** Fibers cross the midline and pass dorsal to the LSO (*inset arrows*). **B.** Ascending Sp5 fibers entering IC via LL (*inset arrows*). Scale bar in A = 500 μm, B = 200 μm.

Figure 6. Bilateral LCIC terminal fields present at P4. **A.** Ipsilateral fibers approach the rostral CNIC before deviating laterally or medially. Terminal zones are not yet modular in appearance but rather enter as a distinct fascicle. Me5 cells are retrogradely labeled on the ipsilateral side due to Me5 efferents present in the sp5 tract projecting to spinal cervical regions. **B.** Contralateral fibers are also present in medial (*inset arrows*) and lateral zones. Some axon collaterals were also observed in the CNIC predominantly towards the rostral pole. **C, D** are

higher magnifications of inset boxes in A, B respectively. Scale bar in A, B = 500 μm; Scale bar in C, D = 200 μm.

Figure 7. Bilateral rostral LCIC terminal fields just caudal to ITN. Axon collaterals are most abundant in these rostral zones. Modular fields, however, remain absent. **A.** Ipsilateral projections appear more punctate and could potentially be traversing the tissue en route to ITN or SC. **B.** Contralateral fibers show full axons with branching collaterals. **C, D** are higher magnifications of inset boxes in A, B respectively. BIC = brachium of IC nucleus, bIC= brachium of IC tract. Scale bar in A, B = 500 μm; Scale bar in C, D = 200 μm.

Figure 8. GAD-positive modules present in layer 2 of LCIC. **A.** GAD-positive zone in LCIC (*inset arrow*). **B.** Higher magnification of inset box in (A). Distinct GAD-positive module is apparent in LCIC layer 2. Discrete modules have not yet fully separated from one another. **C.** High magnification image of ventral most GAD-positive patch in (B). Both cell bodies and terminal puncta are positive for GAD suggesting both GABAergic input and output at the level of LCIC. Scale bar in A = 200 μm; Scale bar in B = 100 μm; Scale bar in C = 30 μm.

Figure 9. Summary schematic comparing multimodal inputs to the IC during early development. This diagram combines data from the present study as well as Fathke & Gabriele (2009), Gabriele, Brunso-Bechtold, & Henkel (2000), Gabriele et al. (2011), and Kandler & Friauf (1993). DCN terminal zones are similar to Sp5 in their distribution to lateral and rostral regions of LCIC, however these fibers do not appear in medial aspects. DCN also projects bilaterally to laminar layers in CNIC along with other previously described inputs (e.g. LSO and DNLL).

Figure 10. Summary of ephrin-B2, EphA4, and ephrin-B3 protein expression. **A, B**. Ephrin-B2 and EphA4 positive (*dashed contours*) LCIC modules, respectively. **C**. Ephrin-B3 extramodular labeling (*negative modules, dashed contours*). Scale bars = 200 μm.

Figures

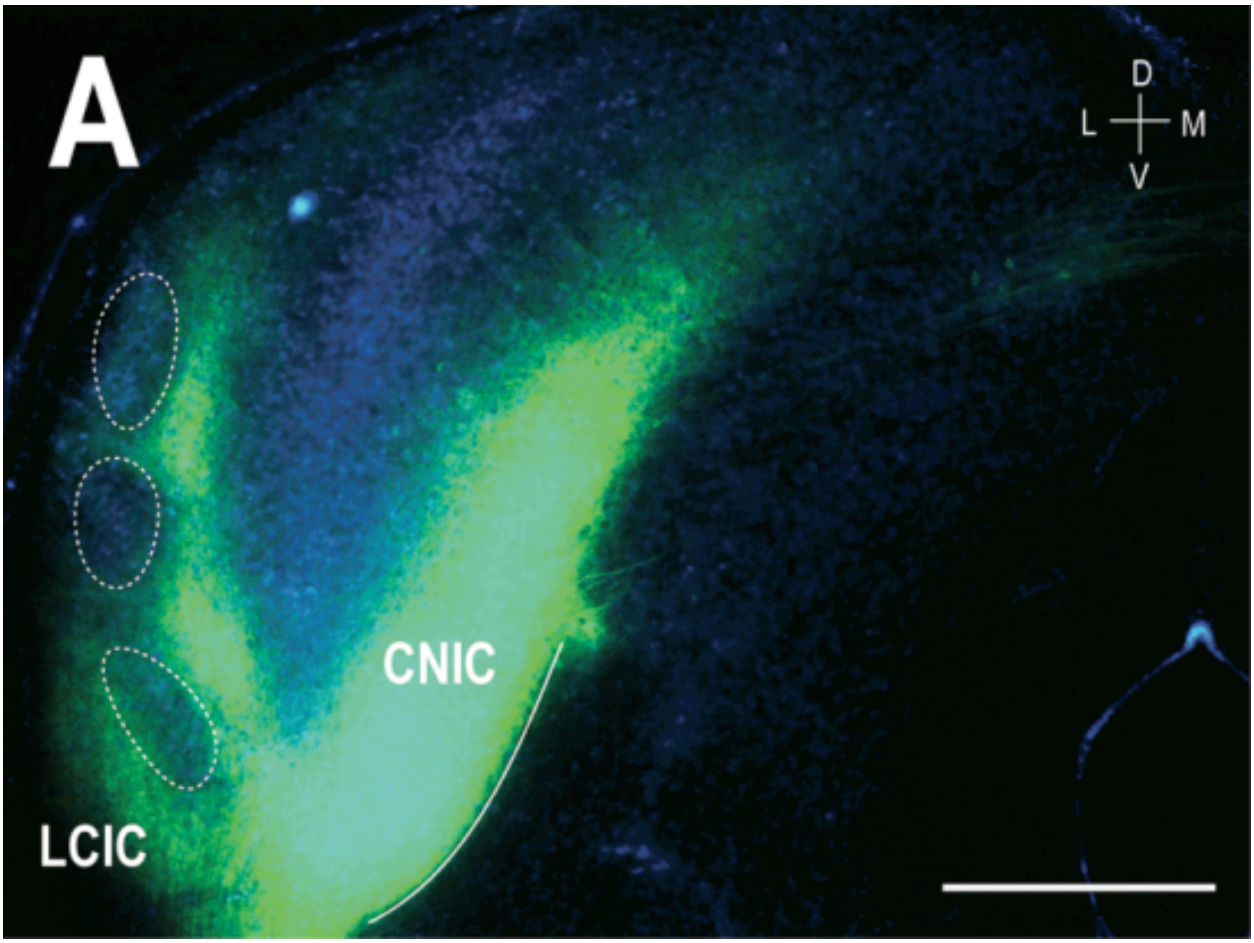

Figure 1.

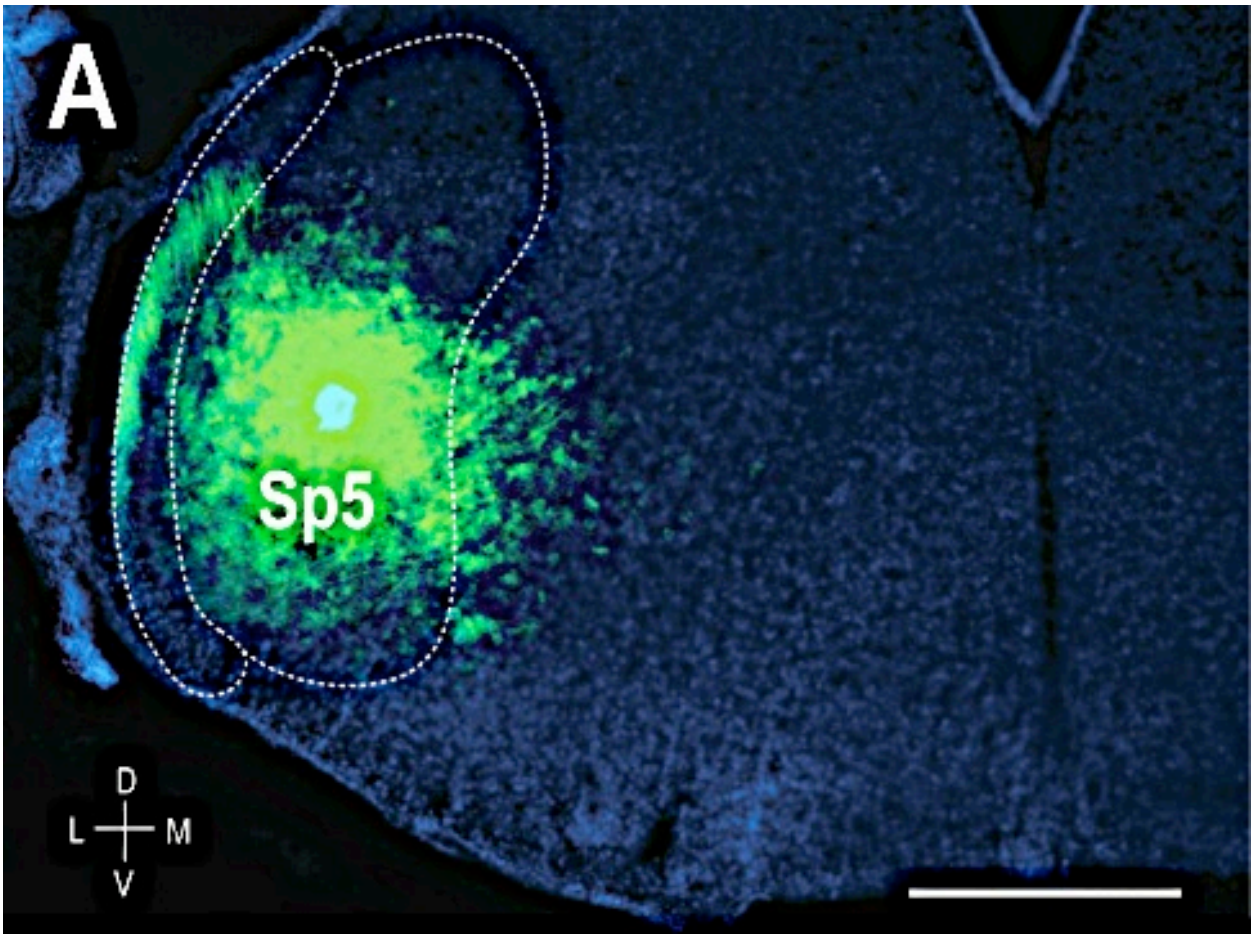

Figure 2.

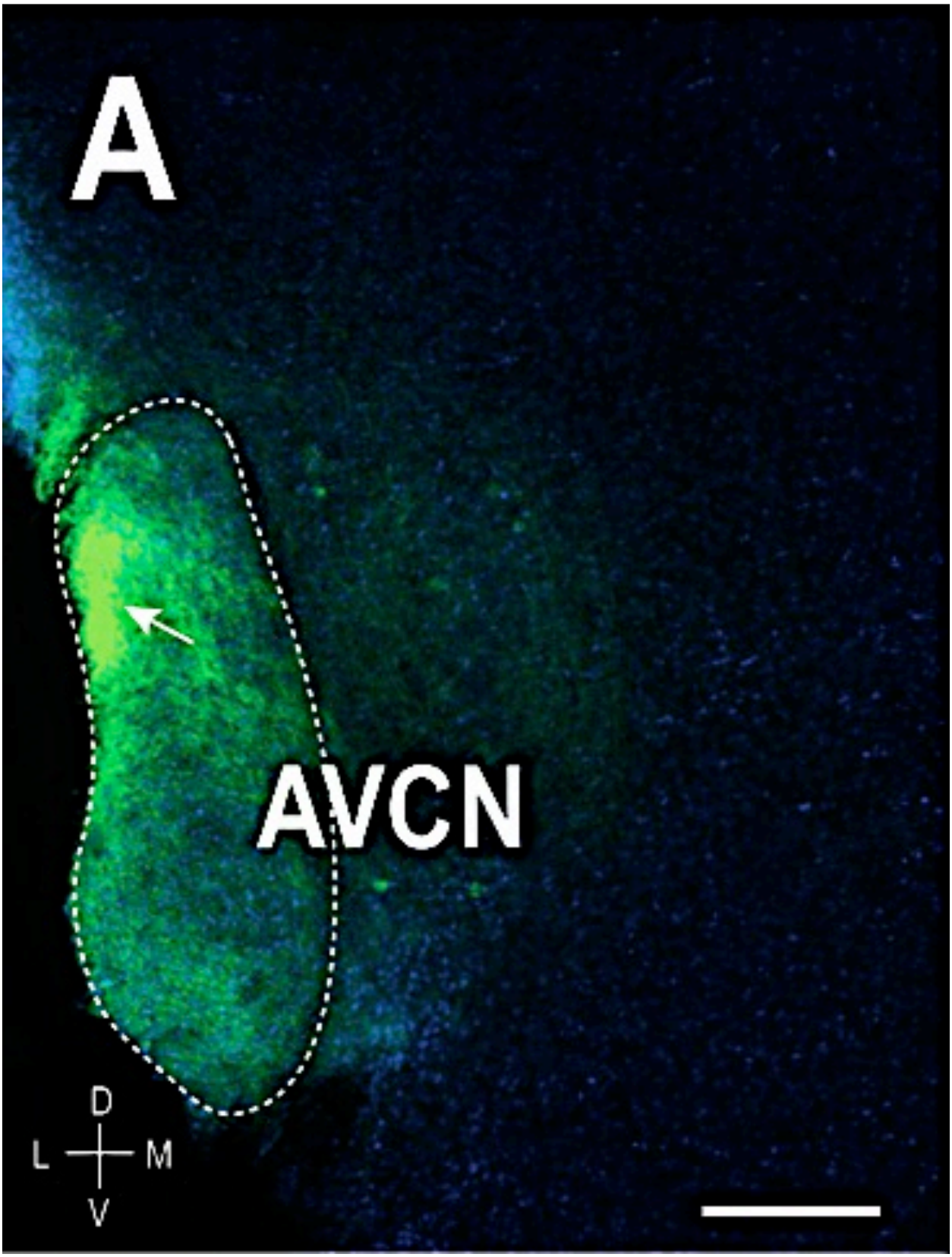

Figure 3.

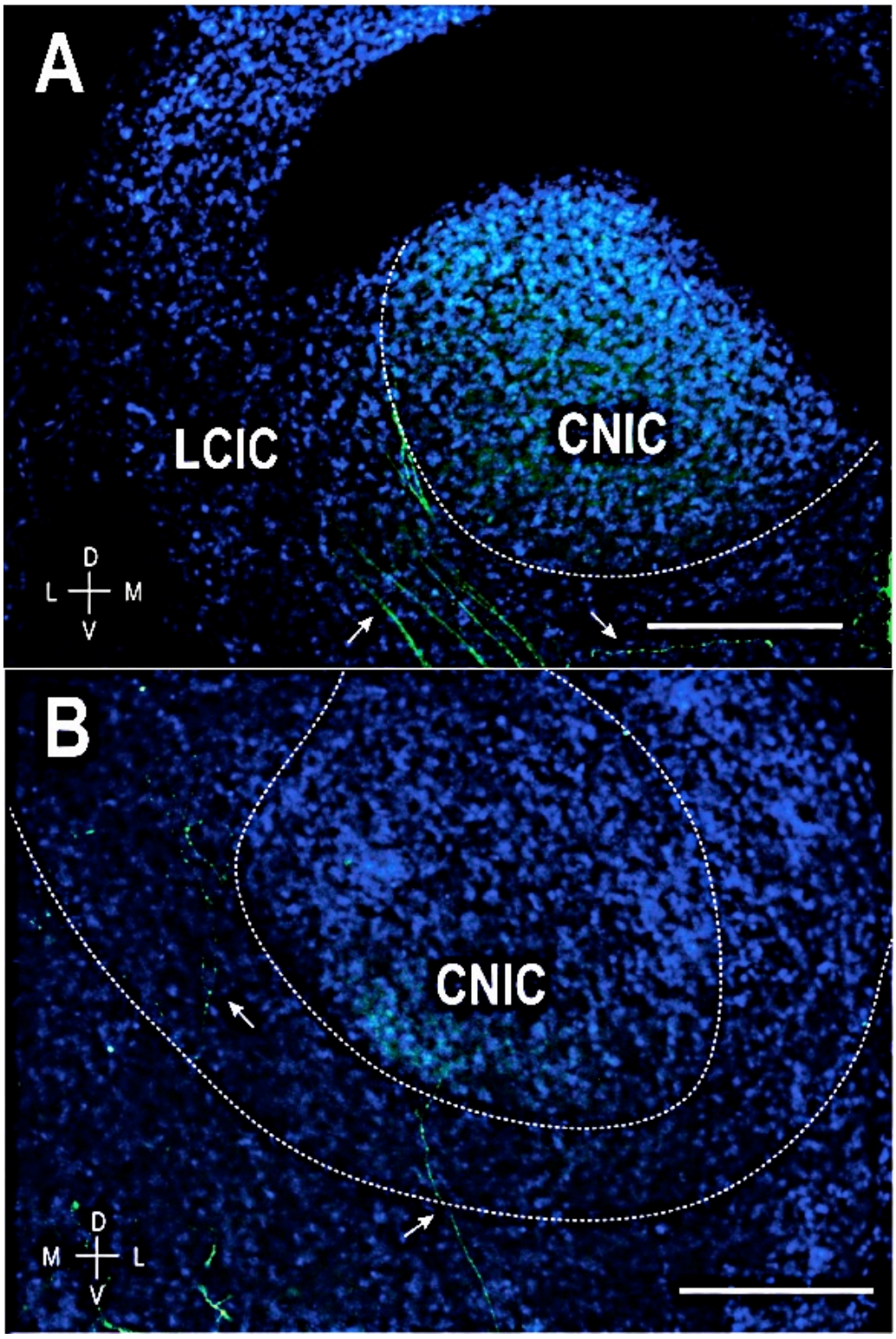

Figure 4.

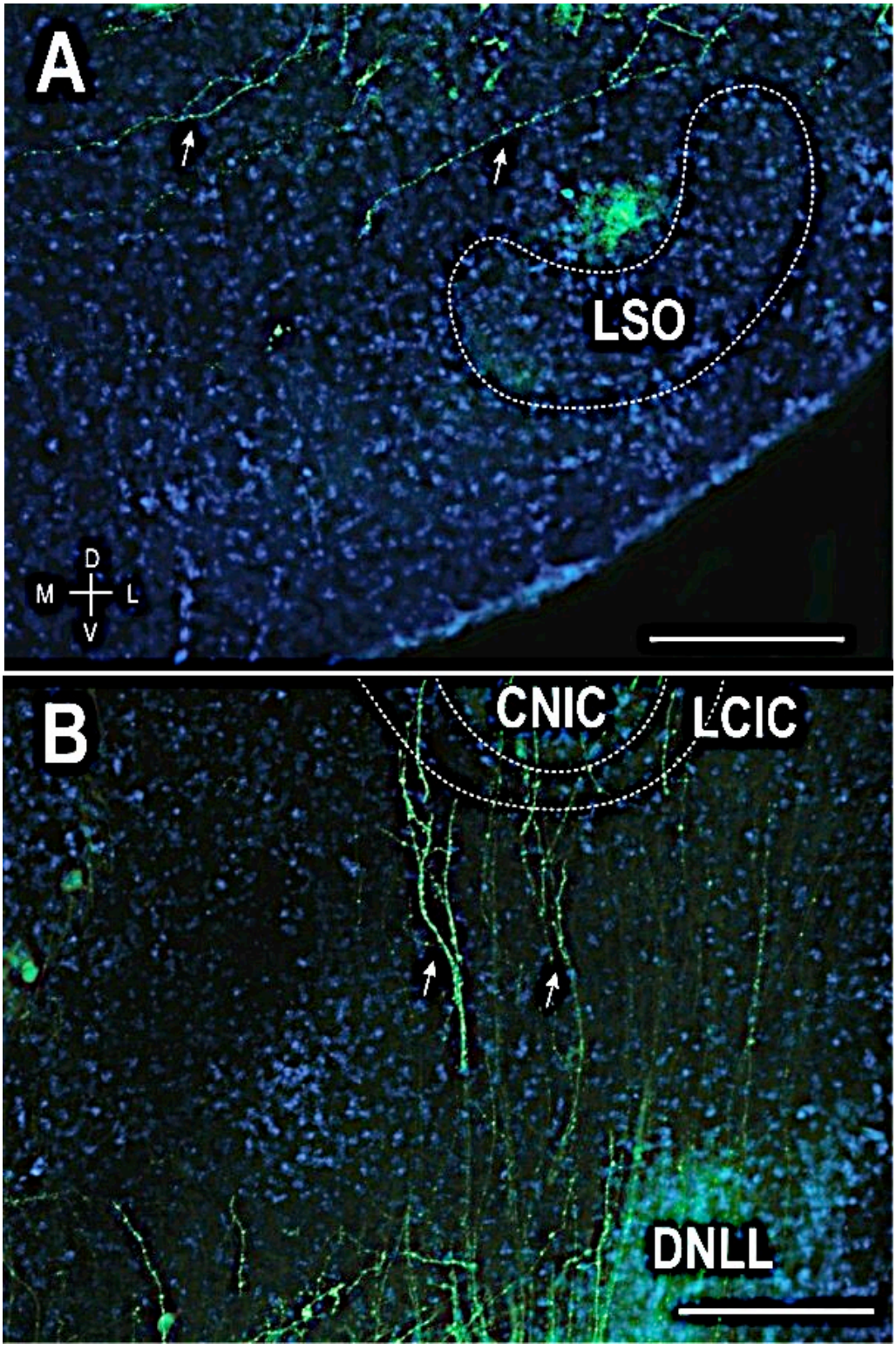

Figure 5.

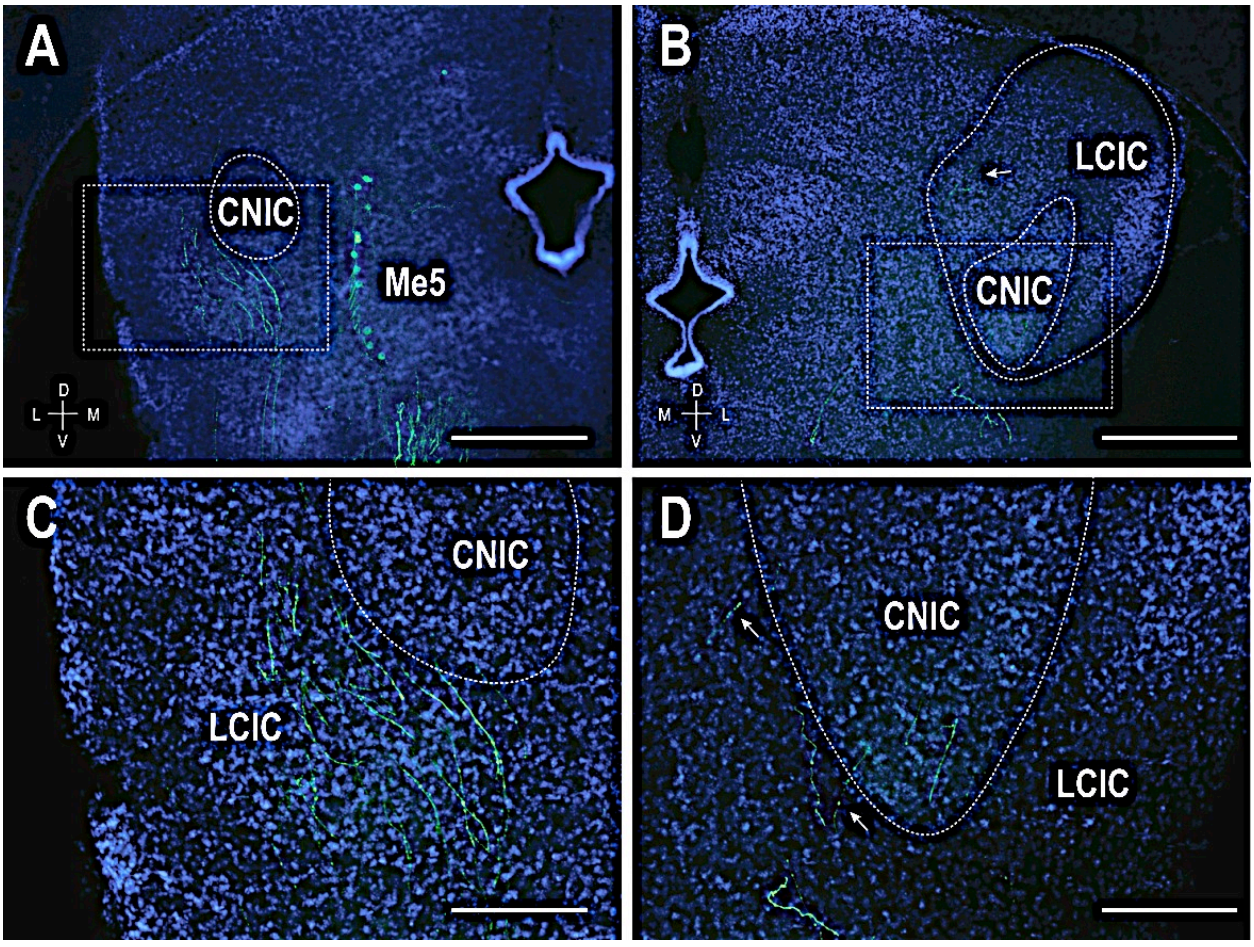

Figure 6.

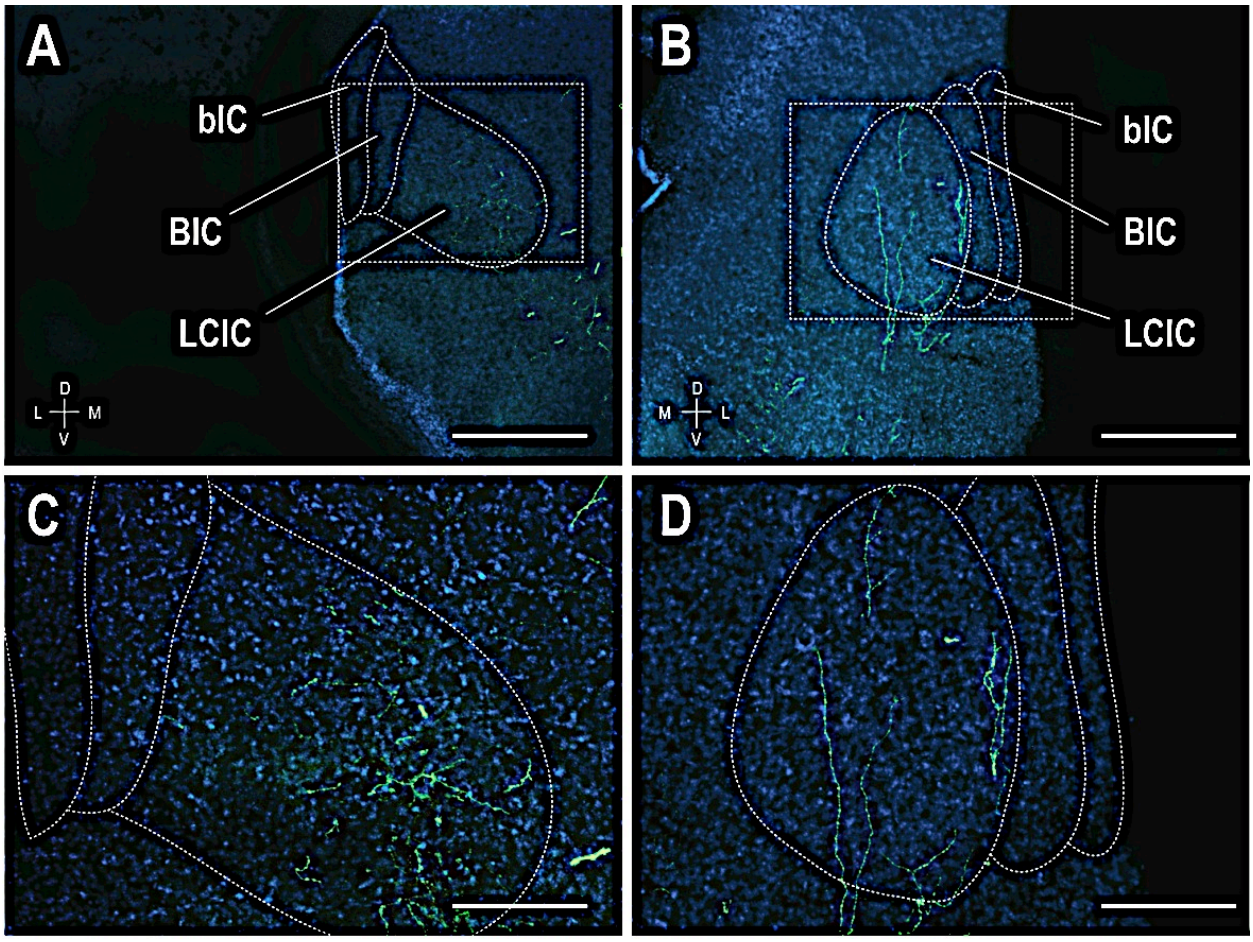

Figure 7.

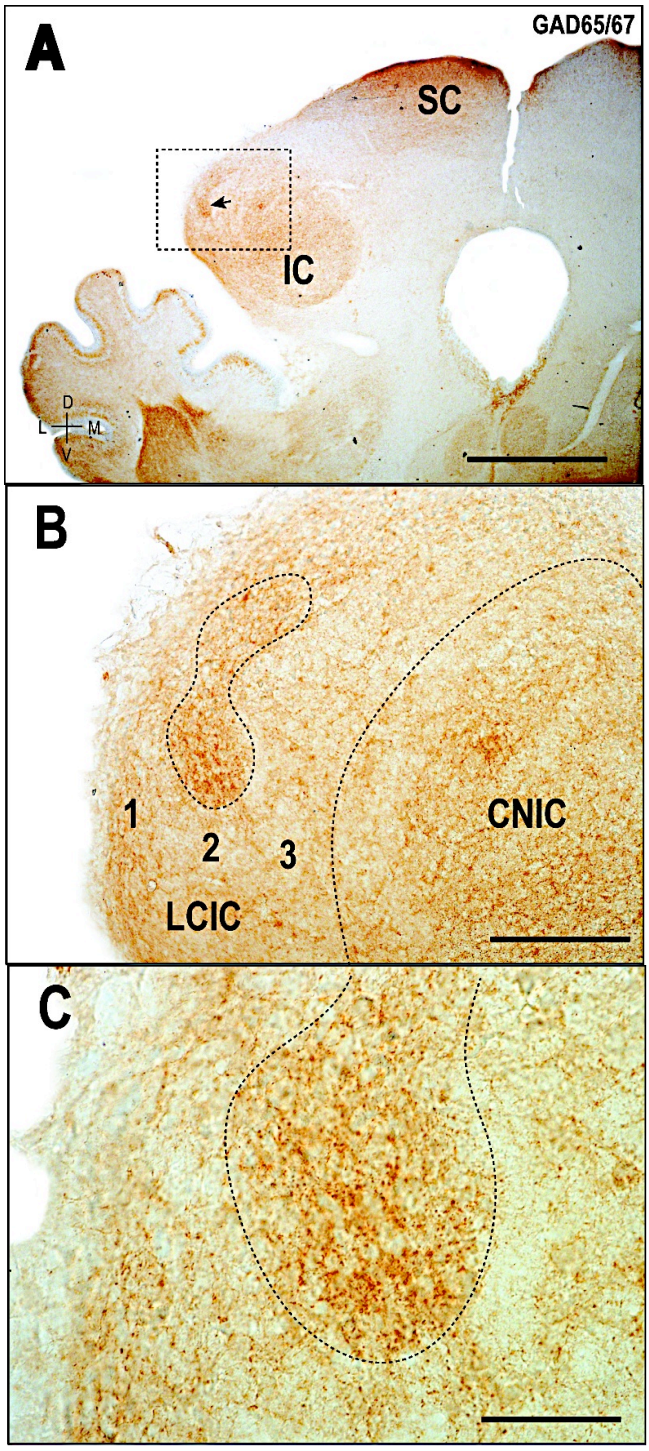

Figure 8.

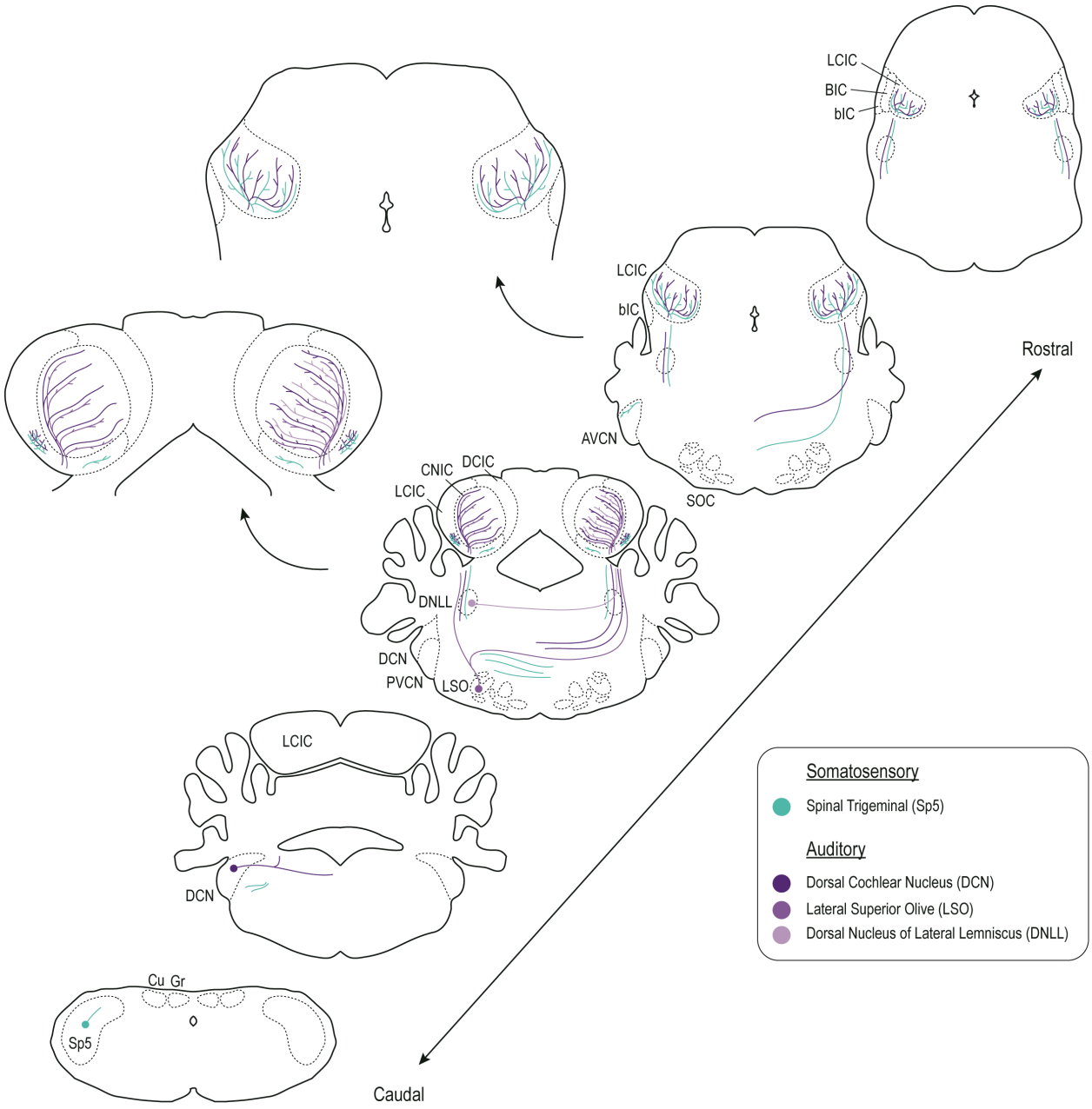
LCIC
BIC
bIC
LCIC
bIC
AVCN
SOC
Rostral
CNIC
DCIC
LCIC
DNLL
DCN
PVCN
LSO
LCIC
DCN
Cu Gr
Sp5
Caudal
Somatosensory
Spinal Trigeminal (Sp5)
Auditory
Dorsal Cochlear Nucleus (DCN)
Lateral Superior Olive (LSO)
Dorsal Nucleus of Lateral Lemniscus (DNLL)

Figure 9.

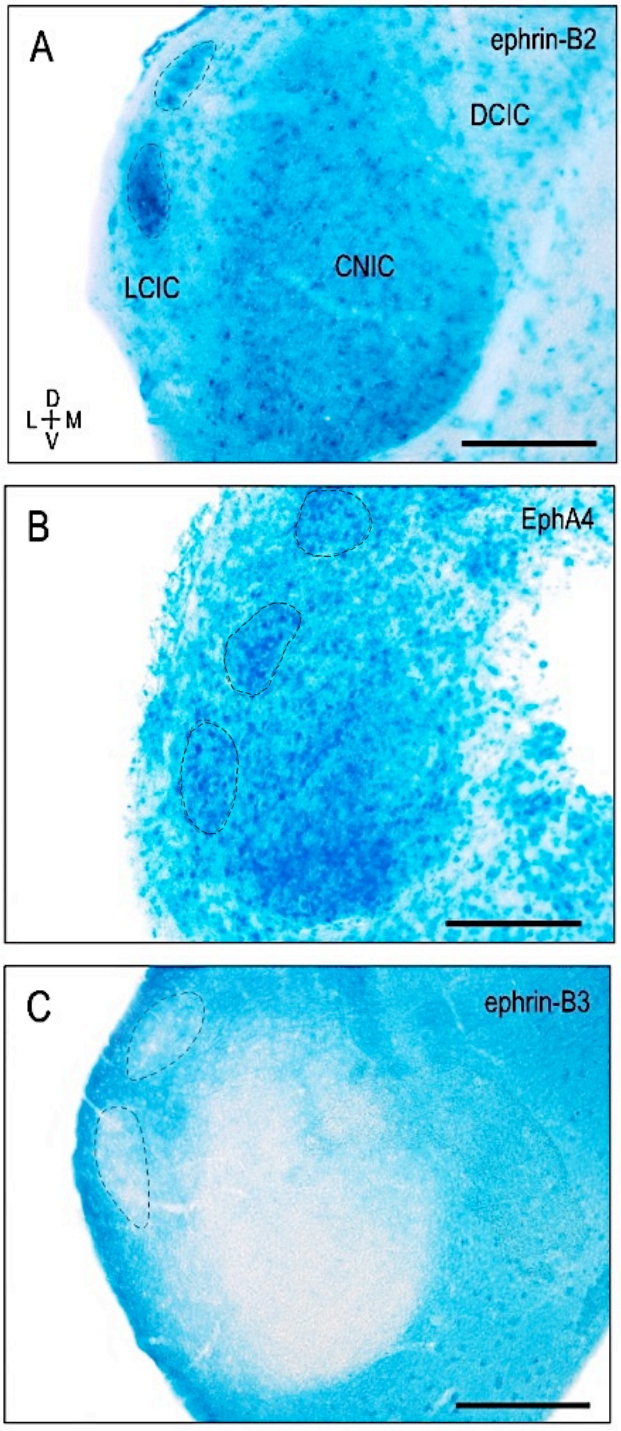

Figure 10.